scientific reports

Check for updates

OPEN

Suppression of the amyloidogenic metabolism of APP and the accumulation of Aβ by alcadein α in the brain during aging

Keiko Honda[1,2,9], Hiroo Takahashi[3,9], Saori Hata[1,2,4,9], Ruriko Abe[2,4], Takashi Saito[5], Takaomi C. Saido[6], Hidenori Taru[1,2], Yuriko Sobu[1,7], Kanae Ando[8], Tohru Yamamoto[3]✉ & Toshiharu Suzuki[1,2,8]✉

Generation and accumulation of amyloid-β (Aβ) protein in the brain are the primary causes of Alzheimer's disease (AD). Alcadeins (Alcs composed of Alcα, Alcβ and Alcγ family) are a neuronal membrane protein that is subject to proteolytic processing, as is Aβ protein precursor (APP), by APP secretases. Previous observations suggest that Alcs are involved in the pathophysiology of Alzheimer's disease (AD). Here, we generated new mouse *App*$^{NL-F}$ (APP-KI) lines with either Alcα- or Alcβ-deficient background and analyzed APP processing and Aβ accumulation through the aging process. The Alcα-deficient APP-KI (APP-KI/Alcα-KO) mice enhanced brain Aβ accumulation along with increased amyloidogenic β-site cleavage of APP through the aging process whereas Alcβ-deficient APP-KI (APP-KI/Alcβ-KO) mice neither affected APP metabolism nor Aβ accumulation at any age. More colocalization of APP and BACE1 was observed in the endolysosomal pathway in neurons of APP-KI/Alcα-KO mice compared to APP-KI and APP-KI/Alcβ-KO mice. These results indicate that Alcα plays an important role in the neuroprotective function by suppressing the amyloidogenic cleavage of APP by BACE1 in the brain, which is distinct from the neuroprotective function of Alcβ, in which p3-Alcβ peptides derived from Alcβ restores the viability in neurons impaired by toxic Aβ.

Alzheimer's disease (AD) is the most common neurodegenerative disease accompanied by brain pathologies such as senile/amyloid plaques and neurofibrillary tangles in the aged population[1,2]. These hallmarks evoke synaptic impairment and neuroinflammation, which induce the progressive loss of memory and cognitive functions[3]. Through various analyses of familial AD (an autosomal dominant hereditary of AD) and sporadic AD in the last three decades, understandings of AD pathobiology progressed and causative genes, *APP* and *PSENs*, and risk factors were identified[4,5]. Among them, the *APP* gene encodes amyloid β-protein precursor (APP), from which neurotoxic Aβ peptides generate, and *PSENs* encode presenilin 1 and 2 (PS1 and PS2), the catalytic protein of γ-secretase complex to cleave APP and to generate Aβ[6,7] (Fig. 1A). Pathogenic mutations on these genes in familial AD increase the generation of neurotoxic and longer Aβ species such as Aβ42[8–11]. Interestingly, the protective mutation of *the APP* gene decreases Aβ generation by increasing an amyloidolytic cleavage

[1]Laboratory of Neuroscience, Graduate School of Pharmaceutical Sciences, Hokkaido University, Sapporo 060-0812, Japan. [2]Advanced Prevention and Research Laboratory for Dementia, Graduate School of Pharmaceutical Sciences, Hokkaido University, Sapporo 060-0812, Japan. [3]Department of Molecular Neurobiology, Faculty of Medicine, Kagawa University, Miki-cho 761-0793, Japan. [4]Bioproduction Research Institute, National Institute of Advanced Industrial Science and Technology (AIST), Sapporo 062-8517, Japan. [5]Department of Neurocognitive Science, Institute of Brain Science, Nagoya City University Graduate School of Medical Sciences, Nagoya 467-8601, Japan. [6]Laboratory for Proteolytic Neuroscience, RIKEN Center for Brain Science Institute, Wako 351-0198, Japan. [7]Laboratory of Neuronal Regeneration, Graduate School of Brain Science, Doshisha University, Kyotanabe 610-0394, Japan. [8]Department of Biological Sciences, Graduate School of Science, Tokyo Metropolitan University, Hachioji, Tokyo 192-0397, Japan. [9]These authors contributed equally: Keiko Honda, Hiroo Takahashi and Saori Hata. ✉email: yamamoto.toru@kagawa-u.ac.jp; suzuki_t@tmu.ac.jp

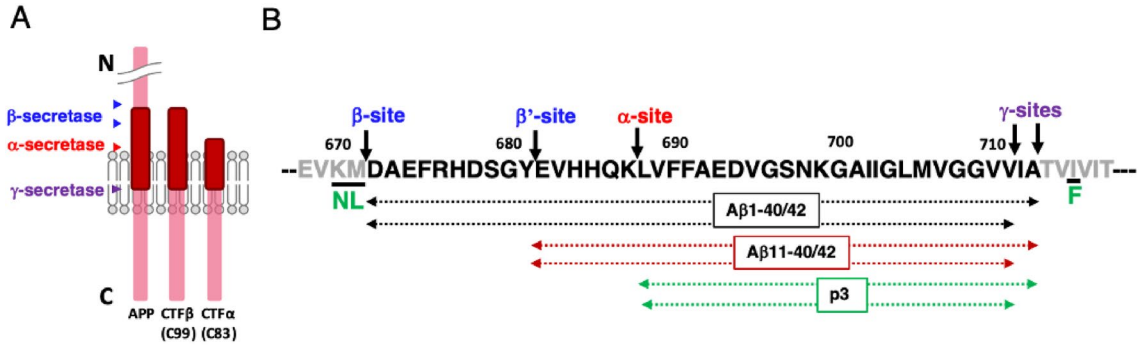

Figure 1. Schematic summary of APP CTFs generated by cleavages of α- and β- secretases and the amino acid sequence of Aβ species. (**A**) APP and the APP carboxy-terminal fragments (CTFβ/C99 and CTFα/C83), which are generated following the cleavage of APP by secretases, are schematically shown. Arrowheads indicate the cleavage site by β-secretase/BACE1, α-secretase (ADAM10/17), and γ-secretase. (**B**) The amino acid sequence of Aβ species generated from CTFs by cleavage of γ-secretase, and the cleavage sites by secretases are shown. $App^{NL\text{-}F/NL\text{-}F}$ (APP-KI) mice harbor the Swedish mutation (K670N/M671L) and the Iberian mutation (I716F), which are indicated in green letters, along with the humanization of three amino acids in Aβ sequence (G676R, F681Y and R684H). These amino acid substitutions generate CTFβ and Aβ1-42/Aβ42 dominantly.

of APP at β'-site by β-site APP-cleaving enzyme 1 (BACE1/β-secretase)[12,13]. Following the cleavage of APP at β-site by BACE1, γ-secretase cleaves the membrane-associated APP carboxyterminal fragment (APP CTFβ) to secrete Aβ species[6,14]. The generation of Aβ is believed to most the primary trigger of neurodegeneration in AD, and the formation of Aβ oligomers is strongly believed to evoke neurodegenerative pathways such as synaptic impairments and neuroinflammation in AD[3,15]. Because most AD patients are sporadic, and they don't carry any pathogenic mutations on causative genes, therefore the molecular regulation of APP metabolism including Aβ generation was widely studied to reveal the pathogenesis of sporadic AD. APP and its cleaving enzymes/secretases are all membrane-associated proteins. Therefore, the generation of Aβ is closely associated with the intracellular trafficking and/or membrane micro localization of APP and secretases, which are regulated by various protein factors[16–19].

We previously identified X11-like (X11L) or APP-binding protein2 (APBA2), one of the factors associated with the trafficking and metabolism of APP in neurons[20–24]. Neuronal cytoplasmic adaptor protein X11L is known to interact with many membrane proteins and regulate their intracellular trafficking and localization[25–28]. Alcadein α (Alcα) was isolated as one of X11L-binding protein[29] and the Alcα formed a tripartite complex with APP through X11L to regulate APP metabolism[30]. Alcadeins (Alcs)/calsyntenins (Clstns) are type I transmembrane proteins as likely as APP, expressed exclusively or mostly in neurons, and there are three family proteins composed of Alcadein α (Alcα/Clstn1), β (Alcβ/Clstn3), and γ (Alcγ/Clstn2) encoded by separate genes[29,31]. Alcα/Clstn1 serves in membrane trafficking as a cargo receptor of kinesin-1[16,32–39]. Alcβ/Clstn3 acts as synaptic adhesion and/or synaptogenesis[40–42], and its γ-secretase product peptide, p3-Alcβ[43], expresses an activity to restore the neuronal viability impaired by Aβ42 toxicity[44]. Alcγ/Clstn2 may be involved in memory performance and cognition[45,46], whose expression is lower in the adult brain compared to the other family proteins[47].

We previously generated Alcα- and Alcβ-deficient (Alcα-KO and Alcβ-KO) mice and analyzed endogenous APP metabolism in these gene knock-out mice brains[48]. Alcα-KO mice enhanced the amyloidogenic metabolism of APP and increased the generation of Aβ. We also analyzed amyloid plaque formation in the brain by generating human APPswe (APP23) transgenic and Alcα-KO double mutant mice (APP23/Alcα-KO)[48]. However, in a previous study, we could not quantify Aβ accumulation and amyloid plaque formation through the aging process, because APP23 mice suddenly died during aging, which makes it difficult to keep sufficient numbers of the aged-mouse population for analyses. This time, we introduced human APP-knock-in mice ($App^{NL\text{-}F/NL\text{-}F}$)[49] to generate new mice lines, Alcα-deficient APP-KI (APP-KI/Alcα-KO) and Alcβ-deficient APP-KI (APP-KI/Alcβ-KO) mice. These mice were analyzed for humanized Aβ generation and amyloid plaque formation in the brain through the aging process. Comparative analyses among three AD mouse models, APP-KI/WT, APP-KI/Alcα-KO and APP-KI/Alcβ -KO, reveal that Alcα regulates amyloidogenic processing of APP and Aβ generation in the brain. The neuroprotective procedures by Alcα are different from the contribution of Alcβ whose secreted peptide p3-Alcβ opposes neuronal toxicity by Aβ oligomers[44,50].

Results

Brain Aβ accumulation in APP-KI, APP-KI/Alcα-KO, and APP-KI/Alcβ-KO mice through the aging process

Schematic pictures of APP cytoplasmic terminal fragments/CTFs, which are generated from APP by cleavage of α- or β- secretase, and the amino acid sequence of Aβ species, which are generated from CTFs by cleavage of γ-secretase, are shown (Fig. 1). Neurotoxic Aβ1-42 is generated by serial cleavages of APP at β- and γ- sites. APP-KI ($App^{NL\text{-}F/NL\text{-}F}$) mice include the Swedish mutation (K670N/M671L) at the amino-terminal of the β-secretase cleavage site and the Iberian mutation (I716F) closed to the γ-secretase cleavage site. Furthermore, the amino acid sequence of Aβ domain was humanized with amino acid substitutions of G676R, F681Y and R684H[49]. Induction of the Swedish mutation increases β-site cleavage[14] with remarkable decreases of β'-site cleavage by BACE1, which

increases Aβ1-XX generation[13]. Furthermore, the Iberian mutation increases AβX-42 generation[51]. Therefore, the APP-KI mice generate human Aβ1-42 (assigned as Aβ42) dominantly rather than Aβ1-40 (assigned as Aβ40).

Hippocampus plus cerebral cortex regions of three mice models, $App^{NL\text{-}F/NL\text{-}F}$ (APP-KI/WT), $App^{NL\text{-}F/NL\text{-}F}$/Alcα-KO (APP-KI/Alcα-KO) and $App^{NL\text{-}F/NL\text{-}F}$/Alcβ-KO (APP-KI/Alcβ-KO) at the indicated ages (4-, 6-, 12- and 15- month-old) were homogenized in TBS, the TBS-insoluble fraction was further solubilized with guanidine-HCl, and Aβ42 in the guanidine fraction was quantified with sELISA (Fig. 2). Accumulation of Aβ42 in brains exponentially increased by 12-month-old in three lines of mice. In 6-month-old mice, Aβ42 amounts increased ~ tenfold in 4-month-old mice for all lines and the increase of Aβ42 continued by 12-month-old, in which the Aβ42 accumulation reached to almost 20- to 30-fold of 6-month-old. However, the accumulations were twice or less in 15-month-old mice brains compared to the brains of 12-month-old mice, suggesting a slowing down of Aβ accumulation in aged mice (15-month-old) of all three lines (Fig. 2A).

Among three mice lines, the magnitude of Aβ accumulation was significantly higher in APP-KI/Alcα-KO mice compared to APP-KI/WT and APP-KI/Alcβ-KO mice at every age, 4-, 6-. 12-, and 15- month-old (Fig. 2B). No significant differences were observed between APP-KI/WT and APP-KI/Alcβ-KO in the level of brain Aβ42

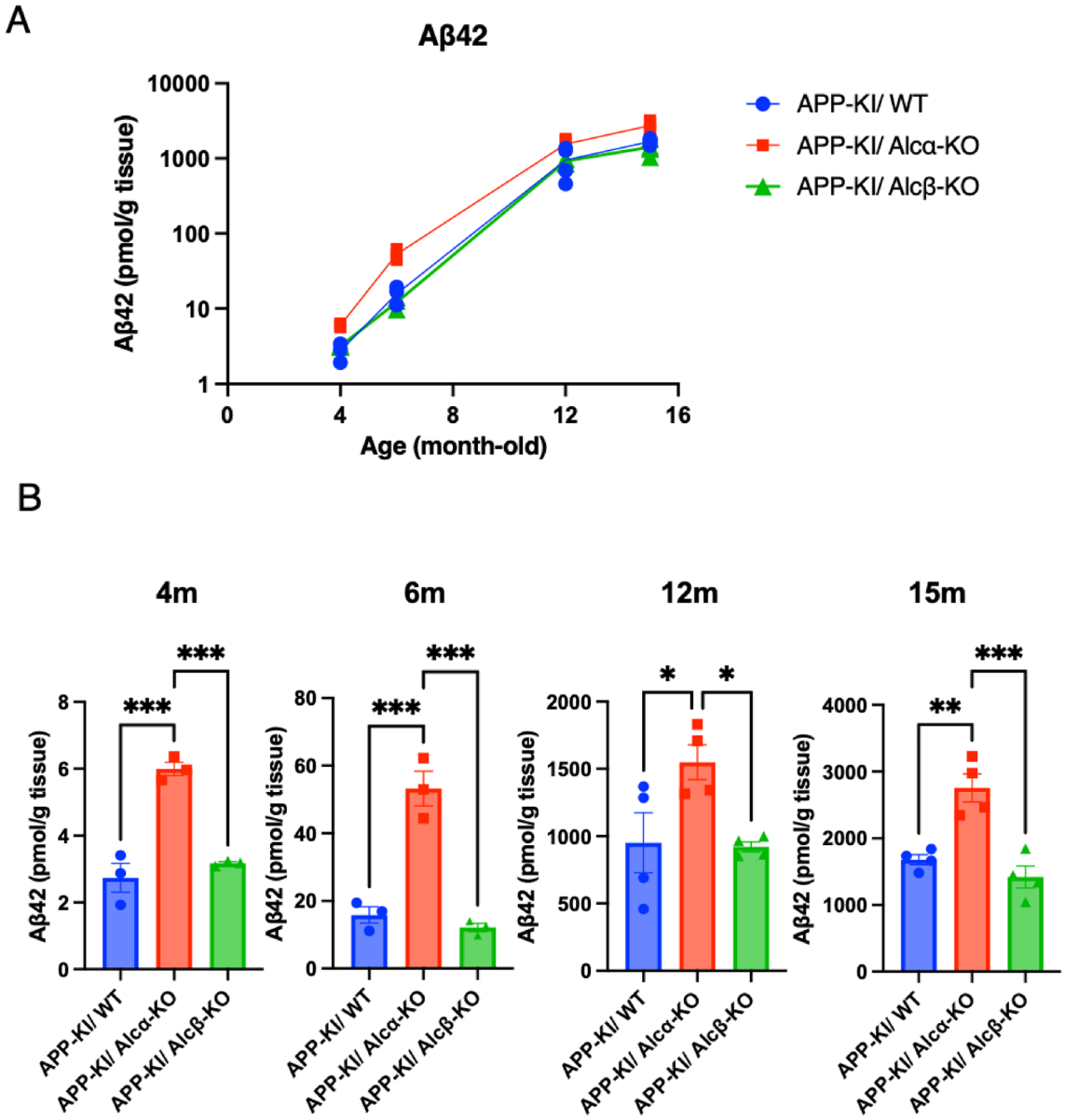

Figure 2. Aβ42 accumulation in the brain of APP-KI/Alc-KO mice models through the aging process. (**A**) Brain Aβ42 levels of APP-KI/WT (circle), APP-KI/Alcα-KO (square), and APP-KI/Alcβ-KO (triangle) mice at 4-, 6-, 12-, and 15- month-old were examined and indicated with semi-log graph. (**B**) The Aβ42 amounts are compared among three mice models at indicated ages. TBS insoluble fraction of cerebral cortex and hippocampus regions was solubilized in guanidine-HCl solution, and Aβ42 was quantified with sELISA. Statistical significance was determined by one-way ANOVA with Tukey's post hoc test for multiple comparisons (means ± S.E.; n = 4. *$p < 0.05$, **$p < 0.01$, ***$p < 0.001$).

accumulation. The age-dependent significant increase of the Aβ42 observed in APP-KI/Alcα-KO mice was not observed in endogenous Aβ42 of Alcα-KO mice[48], in which almost the same levels of Aβ42 were observed at 2-, 6- and 12- month-old respectively, although the respective levels were higher than those of wild-type mice. This difference is due to that only humanized Aβ, but not mouse non-aggregable endogenous Aβ, accumulates in the brain of mice models. The results support that generation of Aβ42 is enhanced in the brain of Alcα-deficient mice regardless of age, and the increasing accumulation of Aβ42 in APP-KI/Alcα-KO mice with age depends on the aggregative prone of human Aβ42.

Amyloid plaque formation in APP-KI/WT, APP-KI/Alcα-KO and APP-KI/Alcβ-KO mice through the aging process

A significant increase of Aβ42 accumulation in APP-KI/Alcα-KO mice suggests the remarkable increase of amyloid plaques in APP-KI/Alcα-KO mice compared to APP-KI/WT and APP-KI/Alcβ-KO mice at 6-, 12- and 15- month-old. Therefore, we next examined amyloid plaque formation by immunostaining of brain slices (Fig. 3). Coronal sections of brain regions including the cerebral cortex and hippocampus of APP-KI/WT, APP-KI/Alcα-KO and APP-KI/Alcβ-KO mice at 6-, 12-, and 15- month-old were immunostained with anti-human Aβ-specific antibody (Fig. 3A–C). All mice models don't show a readily recognizable morphological alteration at these ages. The area of amyloid plaques in three mice models was quantified in brain regions including the cerebral cortex, hippocampus, and entorhinal cortex. The proportion of plaque area was compared among three lines of mice at 6-, 12-, and 15- month-old (Fig. 3D). The amyloid plaque area in 6-month-old mice, as expected from Fig. 2, was less, but the more plaques were detected in APP-KI/Alcα-KO mice brains than in APP-KI/WT and APP-KI/Alcβ–KO mice brains (Fig. 3A, D). The observation is more remarkable in 12-month-old along with increased plaque area, which were almost 10-times more than those of 6-month-old mice (Fig. 3B, D). The amyloid plaque burden may be saturated at 15-month-old because the plaque area became almost the same in three mice models (Fig. 3C, D), which may agree with a trend of saturated Aβ42 accumulation at 15-month-old mice compared to the exponential increase of Aβ42 in younger mice brains (Fig. 2A). In summary, amyloid plaque formation greatly increases in APP-KI/Alcα-KO mice brain by 12-month-old, and the increase of plaques may be saturated in the brains of more aged mice such as 15-month-old mice.

These observations suggest that Alcα deficiency increases the generation and accumulation of Aβ through the aging process, at least by 12-month-old. This was ambiguous in the previous single age-point analysis with 12-month-old APP-Tg (APP23)/Alcα-ko mice[48].

APP cleavage by BACE1 is enhanced in APP-KI/Alcα-KO mice brains

Previous analysis showed that Alcα-deficiency increased β- and β'-sites cleavage of mouse endogenous APP at 2-, 6- and 12-month-old, and this effect was not observed in Alcβ-deficient mice[48]. We further confirmed this by using APP-KI/WT, APP-KI/Alcα-KO, and APP-KI/Alcβ-KO mice brains. Because β'-cleavage of human APP, which generates CTFβ', is reduced by the introduction of Swedish mutation which prioritizes β-cleavage (Fig. 1) and the humanization of amino acids of Aβ region[13], CTFβ which is the product of APP β-site cleavage is more obviously detected in APP-KI mice (Fig. 4). The brain membrane fraction of three mice models was treated with λ-protein phosphatase, which incapacitates for the neuron-specific phosphorylation at Thr668 (numbering for APP695 isoform) of APP and APP CTFs[52,53], to simplify the detection of APP CTF species by immunoblotting[19]. The APP CTFs and APP were analyzed by immunoblotting with antibody raised specific to the APP cytoplasmic region. Using this procedure, we can detect dephosphorylated CTFα (C83) and CTFβ (C99), but not CTFβ'/C89, in the membrane fraction of APP-KI mice brains (see Fig. 1 for APP CTF species).

We detected almost identical levels of CTFα in APP-KI/WT, APP-KI/Alcα-KO, and APP-KI/Alcβ-KO mice at 4-, 6-, 12- and 15- month-old, while significantly increased CTFβ (C99) was detected in APP-KI/Alcα-KO mice at all ages. Amounts of CTFα, CTFβ , and APP were quantified and compared among three mice models at indicated ages (Fig. 4B–D). There were no differences in CTFα levels among three lines of mice at all ages of 4-, 6-, 12- and 15-month-old (Fig. 4B). In contrast to CTFα, CTFβ significantly increased in APP-KI/Alcα-KO mice at 6-, 12- and 15-month-old compared to that of APP-KI/WT mice (Fig. 4C). In younger mice of 4-month-old, the CTFβ also tended to increase in APP-KI/Alcα-KO mice compared to APP-KI/WT mice. Levels of CTFβ in APP-KI/Alcβ-KO mice brains were almost the same as those in APP-KI/WT mice at all ages.

Almost same amounts of APP were expressed in the three mouse lines of all ages (Fig. 4D), except for the comparison of APP-KI/Alcα-KO with APP-KI/Alcβ-KO mice at 12-month-old, which agrees with our previous results that the level of mouse APP was not changed by the deficiency of Alcα or Alcβ[48]. These results coincide with our previous analyses that the cleavages at β- and β'-sites of mouse endogenous APP by BACE1 were enhanced in Alcα-deficient mice brains[48], and indicate that Alcα influences the regulation of amyloidogenic cleavage of APP.

Increase of the CTFβ (C99) in APP-KI/Alcα-KO mice brains was confirmed by separate immunoblotting of the brain membrane fractions (same samples used in Fig. 4) with anti-human Aβ amino-terminal specific antibody 82E1, which reacts to CTFβ but not CTFα (Fig. 5). The brain membrane fraction of three mice models without the treatment of λ-protein phosphatase was used. Two CTFβ bands, the non-phosphorylated CTFβ and the CTFβ phosphorylated at Thr668 (pCTFβ), were detected and the respective band densities were quantified and compared among three mice models at indicated ages (Fig. 5A–C). As can be seen in Fig. 5, the CTFβ and the pCTFβ significantly increased in APP-KI/Alcα-KO mice at the indicated ages compared to those of APP-KI/WT and APP-KI/Alcβ-KO mice. The result confirmed the conclusion shown in the Fig. 4 that the β-cleavage of APP increased in Alcα-deficient mice brains.

Interestingly, the 82E1 antibody detected Aβ, which may be membrane-associated Aβ species. The level of membrane-associated SDS-soluble Aβ increased in APP-KI/Alcα-KO mice compared to APP-KI/WT and APP-KI/Alcβ-KO mice (Fig. 5A and D), which agrees with the increases of the guanidine-HCl soluble Aβ42 (Fig. 2)

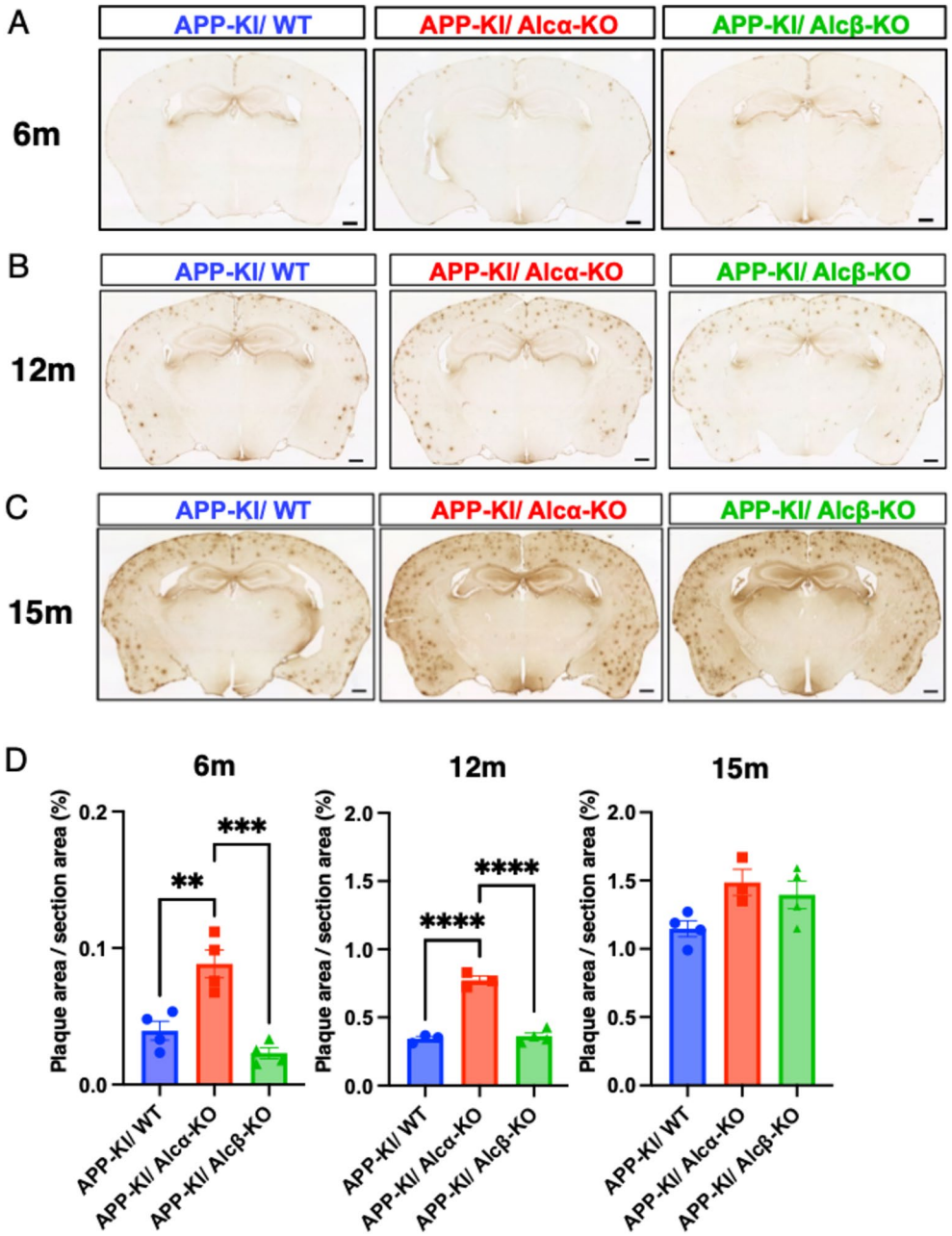

Figure 3. Generation of amyloid plaques in APP-KI/Alc-KO mice models through the aging process. Immunostaining of coronal sections of brain regions including the cerebral cortex and hippocampus of APP-KI/WT, APP-KI/Alcα-KO, and APP-KI/Alcβ-KO mice are shown with the quantification of plaque formation (bar graph). (**A**) 6-month-old, (**B**) 12-month-old, and (**C**) 15-month-old are indicated. Scale bar, 300 μm (in sections). (**D**) The amyloid plaque levels were quantified in 10 slices of 35-μm-thick sections with 315 μm intervals in one mouse at indicated ages. The sum of plaque pixel numbers in each image was counted with ImageJ, and the resulting numbers were divided by the pixel numbers of the area occupied by the slices. Statistical significance was determined by one-way ANOVA with Tukey's post hoc test for multiple comparisons (means ± S.E.; n = 4. $^{**}p < 0.01$, $^{***}p < 0.001$, $^{****}p < 0.0001$).

and the amyloid plaques (Fig. 3) in APP-KI/Alcα-KO mice. Taken together our previous and current analyses, it is obvious that Alcα plays an important role in the regulation of APP cleavages by β-secretase in brain.

Alcα-deficiency increases the localization of APP into endolysosomal pathways where BACE1 localizes actively in neurons

To explore the mechanism of how the brain of APP-KI/Alcα-KO mice model increases β-cleavage of APP, we asked about the intracellular localization of APP and BACE1 in the primary cultured neurons prepared from the

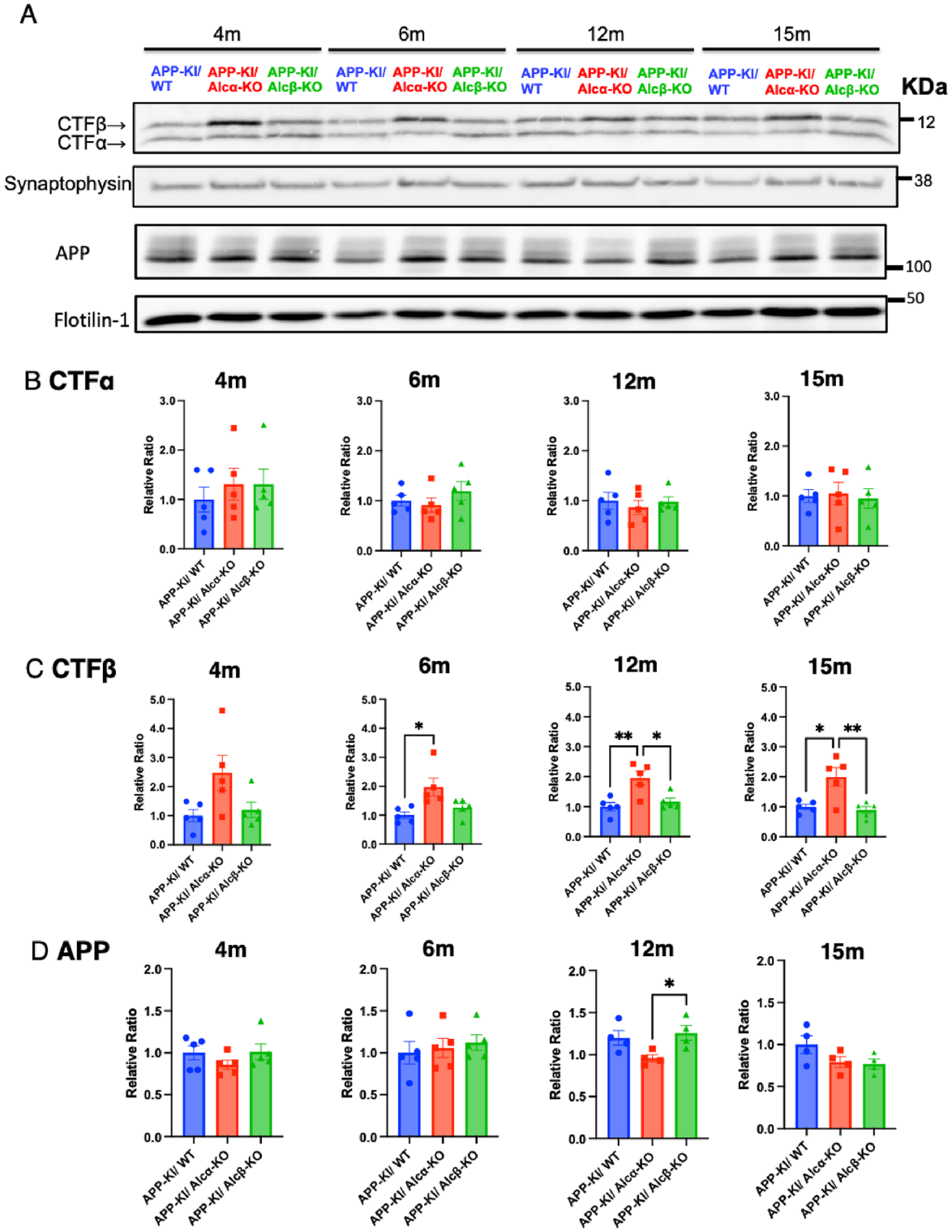

Figure 4. Enhanced amyloidogenic cleavage of APP in APP-KI/Alcα-KO mice. (**A**) Immunoblot analysis of APP CTFs and APP of APP-KI/WT, APP-KI/Alcα-KO, and APP-KI/Alcβ-KO mice brains. Membrane fraction (10 μg protein) of the cerebral cortex plus hippocampus region of mice at 4-, 6-, 12-, and 15- month-old was analyzed by immunoblotting with anti-APP cytoplasmic antibody (to detect both APP CTFs and APP), and anti-synaptophysin and anti-flotillin-1 antibodies. Dephosphorylated APP CTFs and APP are indicated. Numbers (kDa) indicate protein size markers. A reproducible blot of four independent studies used respective four to five mice (n = 4–5) at each age. (**B**-**D**) Quantification of APP CTFs and APP at indicated ages in the three lines of mice. Band densities of APP CTFα, APP CTFβ and APP were standardized to the densities of synaptophysin for CTFα (**B**) and CTFβ (**C**) and flotillin-1 for APP (**D**). Values of APP-KI/WT mice were assigned as a reference value of 1.0 and compared among three lines of mice; APP-KI/WT, APP-KI/Alcα-KO and APP-KI/Alcβ-KO. Statistical significance was determined by one-way ANOVA with Tukey's post hoc test for multiple comparisons (means ± S.E.; n = 4–5. $^{*}p < 0.05$; $^{**}p < 0.01$).

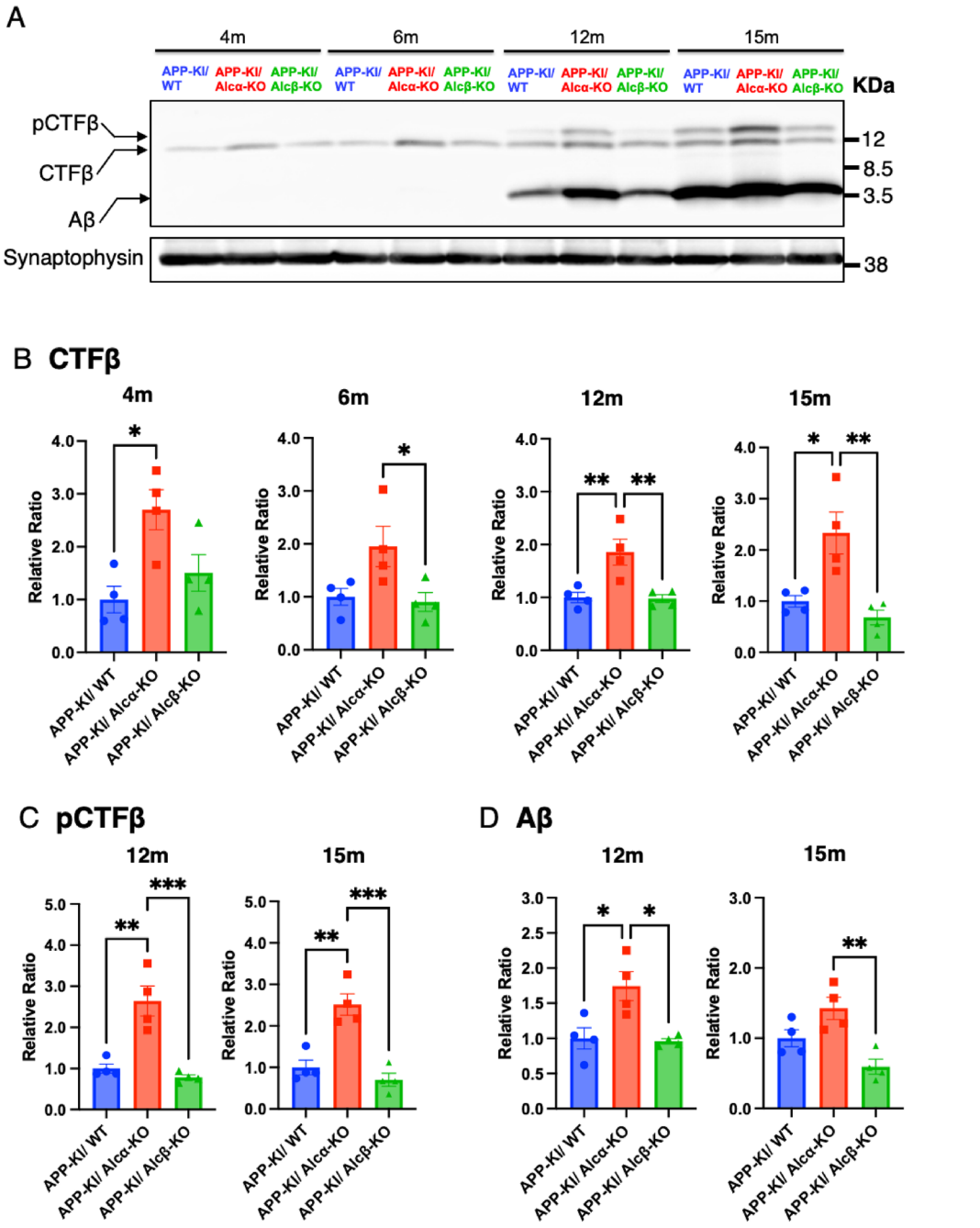

Figure 5. Enhanced APP CTFβ and Aβ generation in APP-KI/Alcα-KO mice. (**A**) Immunoblot analysis of APP CTFβ and Aβ of APP-KI/WT, APP-KI/Alcα-KO, and APP-KI/Alcβ-KO mice brains. Membrane fraction (10 µg protein) of the cerebral cortex plus hippocampus region of mice at 4-, 6-, 12-, and 15- month-old was analyzed by immunoblotting with anti-huma Aβ amino-terminal antibody 82E1(to detect APP CTFβ and Aβ), and anti-synaptophysin antibody. APP CTFβ and pCTFβ (CTFβ phosphorylated at Thr668 of APP695) are indicated with Aβ. Numbers (kDa) indicate protein size markers. A reproducible blot of four independent studies used respective four mice (n = 4) at each age. (**B**-**D**) Quantification of APP CTFs and Aβ at indicated ages in the three lines of mice. Band densities of APP CTFβ, pCTFβ, and Aβ were standardized to the densities of synaptophysin for CTFβ (**B**), pCTFβ (**C**), and Aβ (**D**). Values of APP-KI/WT mice were assigned as a reference value of 1.0 and compared among three lines of mice; APP-KI/WT, APP-KI/Alcα-KO and APP-KI/Alcβ-KO. Statistical significance was determined by one-way ANOVA with Tukey's post hoc test for multiple comparisons (means ± S.E.; n = 4–5. $^{*}p < 0.05$; $^{**}p < 0.01$; $^{***}p < 0.001$).

embryonic brains of mice models and compared the colocalization of APP and BACE1 among APP-KI/WT, APP-KI/Alcα-KO and APP-KI/Alcβ-KO mice models. Primary culture neurons (DIV 14–16) of three mice models were doubly immunostained using a rabbit anti-APP cytoplasmic antibody with mouse anti-BACE1, anti-EEA1 (early endosomal protein), anti-Rab7 (late endosomal protein), and anti-LAMP1 (lysosomal protein) antibodies (Fig. 6A). The colocalization rates of proteins were indicated as Peason's *R*-value (Fig. 6B).

Colocalization of APP with BACE1 is significantly higher in neurons of APP-KI/Alcα-KO compared to those of APP-KI/WT and APP-KI/Alcβ-KO. Interestingly, colocalization of APP with endolysosomal proteins, LAMP, EEA1 and Rab7, also increased in neurons of APP-KI/Alcα-KO compared to those of APP-KI/WT and APP-KI/Alcβ-KO (Fig. 6A and B). The expression levels of APP and BACE1 are almost same among the APP-KI/WT, APP-KI/Alcα-KO, and APP-KI/Alcβ-KO mice brain (Appendex Fig. 1), which were also shown in our previous report[48]. Levels of neuronal synaptophysin were identical in three models, suggesting no remarkable changes of neurons among three mice models. The observation suggests that deficiency of Alcα introduces more APP into the endolysosomal pathway, in which acidic condition activates BACE1. Interestingly, the colocalization of APP with LAMP1 (lysosome marker) and Rab7 (late endosome marker), but not EEA1(early endosome marker), decreased in neurons of APP-KI/Alcβ-KO mice compared to APP-KI/WT mice. We currently don't have a suitable explanation for this. However, at least these observations suggest that Alcα deficiency appears to enhance the transport of APP into the endolysosomal pathway, by which β-cleavage of APP was facilitated in neurons of the APP-KI/Alcα-KO mice model. The results also agree with the previous biochemical analysis that the endogenous APP cleavage at the β-site increases in the endosome-rich fraction of Alcα-KO mice brain[48].

Discussion

Brain Aβ is largely derived from neurons and various neuronal factors involved in the regulation of APP processing including amyloidogenic cleavages were reported[18,19]. Alteration of membrane lipid composition and altered micro-membrane localization of γ-secretase complex in neurons are also involved in the γ-cleavage of APP, which induces qualitative and/or quantitative changes in Aβ generation[54–56]. However, many studies to reveal the regulatory metabolisms of APP were performed by cell-based studies and/or in vitro analysis. Until now, there have not been many studies analyzing the molecular function of these regulatory factors in APP metabolism in vivo except for several factors[21–23,57–59]. Alcα is one of the proteins that are suggested to be associated with AD pathophysiology[43,47,60–62] but there was no obvious evidence of how Alcα is associated with intracellular events linked to AD pathobiology including the regulation of Aβ generation in vivo up to our previous report[48]. Of course, the physiological function of Alcα in intracellular membrane vesicle transport, as does APP, has been well understood in neurons[16,34,36,37,39].

Our present analysis using new mouse models assured our previous evidence that Alcα suppresses the amyloidogenic β-cleavage of APP in vivo. Our study suggests that the increase of β-site cleavage of APP in APP-KI/Alcα-KO mice brains is due to the increased chance of the β-site cleavage of APP in the endolysosomal pathway, which is also supported by our previous observation for endogenous APP metabolism in Alcα-KO mice[48]. Of course, we cannot rule out a possibility that the gene knock-out of Alcα and/or Alcβ proteins may affect the expression of various genes including genes encoding endolysosomal proteins, by which the colocalization of APP with the endolysosomal proteins may change in neurons of APP-KI/Alcα-KO mice. However, at least we have reported that the protein levels of APP and BACE1 in Alcα-KO and Alcβ-KO mice brains are equivalent compared to those of wild-type mouse brains[48], and the same results are also obtained in the present study with brain lysates of APP-KI/Alcα-KO, APP-KI/Alcβ-KO, and APP-KI/WT mice (Appendix Fig. 1). Therefore, our previous and current analyses support the conclusion that the enhanced β-cleavage of APP in Alcα-KO mice brains is due to the increased localization of APP in the BACE1-active region(s) of neurons.

Furthermore, we newly revealed the process of Aβ accumulation in the absence of Alcα expression, which was a constitutive and enhanced amyloidogenic processing of APP and accumulation of Aβ through aging, at least by 12 months. Taken together with our previous results[48], the present analyses certified that Alcα serves to suppress the amyloidogenic processing of APP in neurons, and the possible mechanism is proposed schematically here (Fig. 7). Although our present study was out of focus on cytoplasmic factors that regulate intracellular metabolism and transport of APP, the cytoplasmic factors may contribute to suppression of amyloidogenic metabolism of APP with Alcα. One possible candidate is X11-like/X11L, a neuron-specific member of X11/Mint family proteins[20,28]. Association of the cytoplasmic X11L with APP suppresses amyloidogenic cleavage of APP at β- and β'-sites in vivo[22], and further association of APP with Alcα by mediating X11L to form a tripartite complex (APP-X11L-Alcα) enhances the suppression of the β-cleavage of APP[29,30]. Therefore, it is possible to assume that intracellular trafficking of APP by collaborating with Alcα and X11L secures a non-amyloidogenic metabolism of APP in neurons.

There may be other possible mechanisms that Alcα suppresses β-cleavage of APP. Alcα and APP serve as a cargo receptor of kinesin-1 independently, and the respective cargo receptor plays an important role in intracellular membrane trafficking of specific proteins by kinesin-1 in neurons [16,39,63]. Both Alcα and Alcβ can interact with the kinesin light chain (KLC) of kinesin-1 directly in vitro[34]. There are two KLC-binding WD motifs in Alcα, whereas only one WD motif exists in Alcβ[16,34]. These previous analyses suggest that Alcα cargo vesicles serve in the protein transport by kinesin-1 more important than Alcβ cargo vesicles in the transport of proteins. Deficient of Alcα rather than Alcβ may impair the transport of proteins which play in the regulation of APP metabolism. This may be a reason for the increased amyloidogenic processing of APP in Alcα-deficient mice. Furthermore, several studies suggest that the altered trafficking of organelles is involved in the pathogenesis of Alzheimer's disease[64–66]. In APP-KI/Alcα-KO mice, the aberrant trafficking of endolysosomal compartments may have occurred. We should perform further analysis to reveal the relationship between APP amyloidogenic cleavage and Alcα function in vivo to understand the exact mechanism.

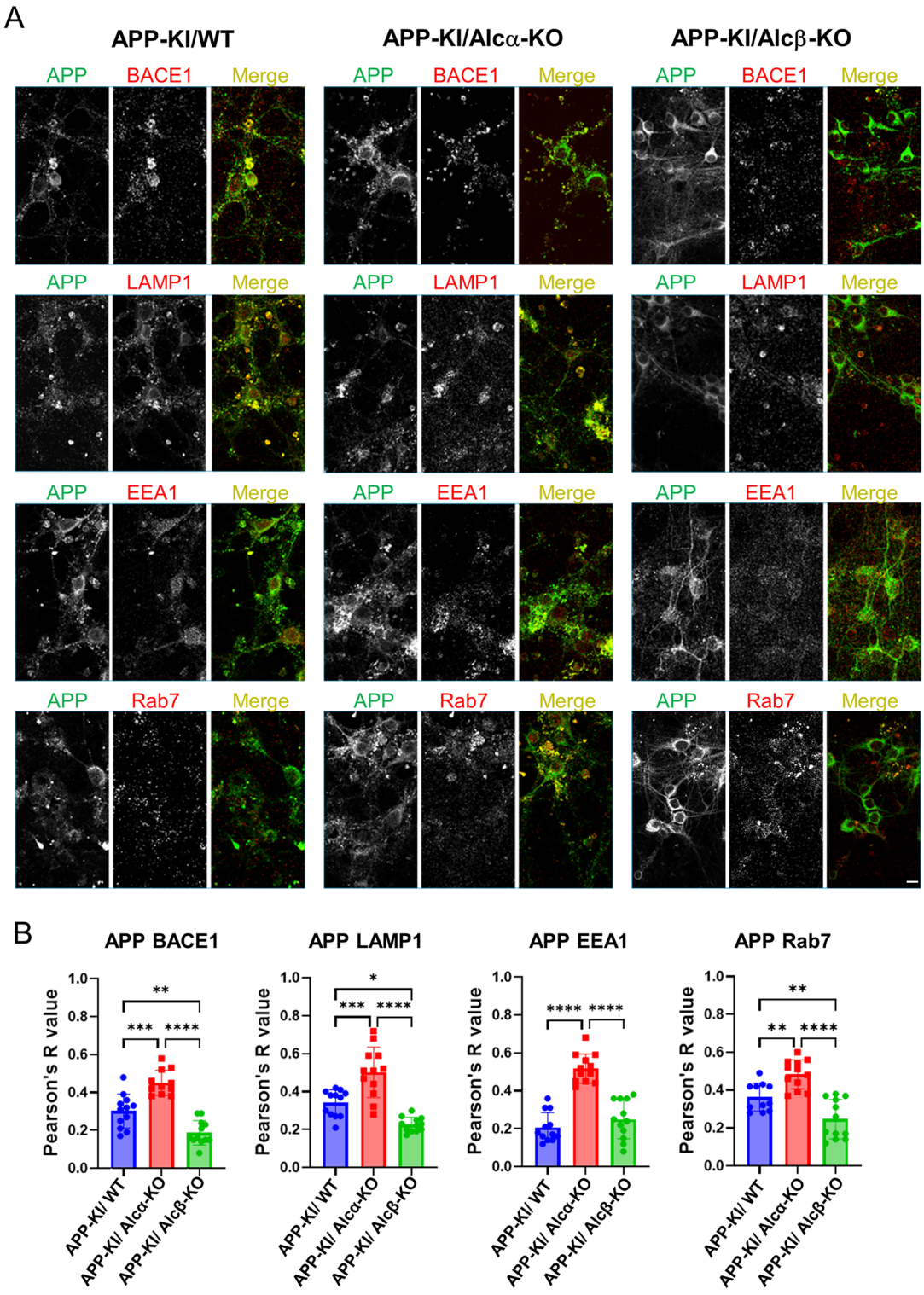

Figure 6. Colocalization of APP with BACE1 and endolysosomal proteins in primary cultured neurons of three mice lines. (**A**) Localization of APP with proteins. Primary cultured neurons (DIV 14–16) of APP-KI/WT, APP-KI/Alcα-KO, and APP-KI/Alcβ–KO mice were immunostained with a rabbit anti-APP antibody (green) together with mouse anti-BACE1, anti-LAMP1, anti-EEA1 or anti-Rab7 antibodies (red). Scale bar, 10 µm. (**B**) The colocalization efficiency of APP with BACE1, LAMP1, EEA1, or Rab7. Colocalization was calculated using the coloc2 plugin in Fiji (ImageJ) with the pixel intensity correlation between each protein and APP indicated as Peason's R value (*R* value of 1.0 indicates perfect colocalization while an *R* value of 0 indicates random localization). Cells were independently prepared in two separate experiments, and for each preparation, six to seven images were acquired. All values were combined and subjected to statistical analysis with indicated numbers of independent biological repeats. Asterisk indicates *$p < 0.05$, **$p < 0.01$, ***$p < 0.001$, ****$p < 0.0001$ ($n = 12 \sim 13$, mean ± S.E.).

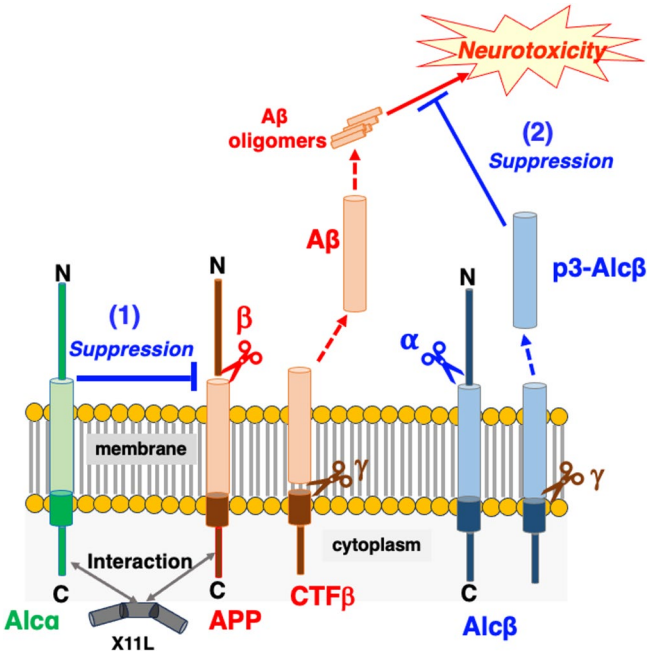

Figure 7. Schematic functions of alcadeins and their metabolic peptide p3-Alc in neuroprotection. Possible roles of Alcα and Alcβ against to Aβ-dependent neurotoxicity are shown. (1) Alcα suppresses amyloidogenic β-cleavage of APP which is also regulated by association with cytoplasmic adaptor proteins such as X11-like/X11L. Association of APP with Alcα mediated by cytoplasmic X11L attenuates the generation of APP CTFβ, a precursor fragment of Aβ. (2) Nonaggregate peptide p3-Alcβ is generated from Alcβ by cleavages of α- and γ-secretases. The p3-Alcβ is known to restore the viability of neurons impaired by Aβ oligomers.

Therefore, in contrast to Alcα, Alcβ is not likely to serve APP processing directly. However, our recent research revealed that the p3-Alcβ peptides, which are generated from Alcβ following the proteolytic cleavages by α- and γ-secretases[43,67], serve to restore neuronal vitality impaired by Aβ42 oligomers in vivo and in vitro[44,50]. Therefore, Alc family proteins, at least Alcα and Alcβ, play an important role in the preservation of a healthy brain from neurodegeneration, respectively (Fig. 7).

Methods

Generation of APP -KI/Alc-KO double-mutant mice

App$^{NL\text{-}F/NL\text{-}F}$ (C57BL/6-App < tm2(NL-F)Tcs, RRID:IMSR_RBRC06343)[49], Alcadein α/Calsyntenin 1 -KO (B6NJcl,Cg-Clstn1 < tm1.1Tymo >, RRID:IMSR_RBRC11513) and Alcadein β/Calsyntein 3 -KO (B6NJclCg-Clstn3 < tm1Tymo >, RRID:IMSR_RBRC11514) mice[48] were housed in a specific pathogen-free (SPF) environment with a microenvironment vent system (Allentown Inc., Allentown, NJ, USA), under a 12 h light and dark cycle and fed with diet and water freely. Respective 3–5 male or female siblings were housed in a cage (floor space 535 cm^2) with a micro barrio top. All animal studies were conducted in compliance with the ARRIVE guidelines and all experimental protocols were approved by the Animal Care and Use committees of Hokkaido University. All methods were performed in accordance with the relevant guidelines and regulations of American Veterinary Medical Association (AVMA) Guidelines for the Euthanasia of Animals (2020). APP-KI/Alcα-KO and APP-KI/Alcβ-KO mice were generated by mating to *App*$^{NL\text{-}F/NL\text{-}F}$ (APP-KI) mice and homologous double-knock-in/knock-out mice were used for experimentation. We used only female mice for all analyses to exclude possible differences between genders.

Extraction and quantification of brain Aβ and APP and its carboxy-terminal fragments

Brain lysate for Aβ assay was prepared as described[23] with some modifications[68]. The cerebral cortex and hippocampus regions of the left half brain were dissected and homogenized in a fourfold volume of TBS (20 mM Tris–HCl, pH 7.4 containing 137 mM NaCl and protease inhibitor cocktail (PIC, 5 µg/mL chymostatin, 5 µg/mL leupeptin, and 5 µg/mL pepstatin) with a Dounce homogenizer (tight) for 30 strokes in ice. The lysate was subject to centrifugation (200,000 × g for 20 min at 4 °C) with TLA 100.4 rotor (Beckman Coulter Life Science, Brea CA, USA). The resulting precipitate was further homogenized in a ninefold volume of TBS with Dounce homogenizer (tight) for 30 strooks and subject to centrifugation (100,000 × g for 20 min at 4 °C) with TLA 55 rotor (Beckman Coulter Life Science). The pellet was dissolved in an equal volume of 6 M guanidine-HCl solution in 50 mM Tris–HCl, pH 7.6 under the sonication (one second with one second interval of 17 cycles, with SONICSTAR85, WAKENYAKU, Co., Kyoto Japan) and stand still for 1 h at room temperature. The sample was subject to centrifugation at 130,000 × g for 20 min with TLA55 rotor and resulted supernatant was used for Aβ40 and Aβ42

assay. Human Aβ40 and Aβ42 were quantified by sandwich ELISA as described previously[69] except that 82E1 antibody (Immuno Biological Laboratories, Fujioka, Japan, Cat 10,323) was used instead of the 2D1 antibody[70].

The cerebral cortex and hippocampus regions of the right half brain were dissected and homogenized in a tenfold volume of buffer H (20 mM HEPES, pH 7.4 containing 150 mM NaCl, 5 mM EDTA, 10% (v/v) glycerol and PIC with Dounce homogenizer (tight) for 30 strokes in ice (crude lysate). An aliquot (200 µl) of the crude lysate was diluted with 200 µl of × 2 RIPA buffer (100 mM Tris–HCl, pH 7.6 including 300 mM NaCl, 2% (v/v) Nonidet P40, 1% (w/v) sodium deoxycholate, 0.2% (w/v) SDS and × 2 PIC), subject to sonication (one second with one second interval of 10 cycles), and centrifugation (12,000 × g for 1 min at 4 °C), and the resultant supernatant was used as total lysate. The remaining crude lysate was centrifuged (1,000 × g for 10 min at 4 °C), and the supernatant (post-nuclear fraction) was further subject to centrifugation (100,000 × g for 1 h at 4 °C) with a rotor (Beckman TLA-55). The resulting precipitate (membrane fraction) was suspended in 300 µl of × 1 RIPA buffer (50 mM Tris–HCl, pH 7.6 including 150 mM NaCl, 1% (v/v) Nonidet P40, 0.5% (w/v) sodium deoxycholate, 0.1% (w/v) SDS and PIC), subject to sonication (one second with one second interval of 15 cycles), centrifuged (12,000 × g for 10 min at 4 °C), and the supernatant (membrane lysate) was used for detection of membrane proteins. Protein amounts were quantified with BCA Protein Assay Kit (Cat T9300A, TAKARA, Kyoto, Japan).

To detect APP and APP CTFs, membrane lysate was diluted with a phosphatase buffer (5 mM Tri-HCl, pH 7.5, 0.1 mM EDTA, 5 mM DTT, 0.1% BRIJ35, 2 mM $MnCl_2$) to the concentration of 1 mg/ml protein, and incubated with 300 unit of λ protein phosphatase (Cat P9614, Sigma-Aldrich) at 30 °C for 4 h, because the phosphorylation of APP cytoplasmic region at Thr668 (amino acid number for APP695 isoform) causes the complex protein pattern on immunoblotting[19,48]. The treated sample (10 µg of protein) was subject to Tris-Tricine poly acrylamide gel (12.5%) electrophoresis for APP CTFs and Tris-Glysin polyacrylamide gel (8%) electrophoresis for APP, and separated proteins were transferred onto nitrocellulose membrane (Cat P/N66485, Paul Corp., Pensacola, FL, USA) for immunoblotting. Membranes were blocked in 5% non-fat dry milk (barcode 4 902,220 354,665, Morinaga Milk Industry, Tokyo, Japan) in TBS-T (20 mM Tris–HCl [pH 7.6], 137 mM NaCl, 0.05%(v/v) Tween 20 (Cat sc-29113, Nacalai Tesque, Kyoto, Japan), probed with the indicated antibodies in TBS-T, and washed with TBS-T. Immunoreactive proteins were detected using Clarity Western ECL substrate (Cat 1,705,061, Bio-Rad, Hercules, CA, USA) and quantitated on a LAS-4000 (FUJIFILM, Tokyo, Japan). The protein levels detected and quantified were standardized with the levels of flotillin 1 or synaptophysin because both proteins don't change their levels in the brain of Alcα-KO and Alcβ-KO mice compared to WT mice's brain[48]. Anti-APP antibody 369 (1:5000 dilution)[52], anti-flotillin-1 (1:1,000; BD Transduction Laboratories), anti-synaptophysin (1:1000, D-4, Cat sc-17750, Sant Cruz Biotechnology, Dallas, TX, USA), anti-mouse IgG HRP-Linked F(ab') 2 Fragment sheep (1:10,000 dilution Cat NA9310, Cytiva, Mariborough, MA, USA) and anti-rabbit IgG HRP-Linked F(ab') 2 Fragment donkey (1:10,000 dilution Cat NA9340, Cytiva) were used.

In a separate study, to detect APP CTFβ, the membrane lysates (10 µg of protein) without the treatment of λ protein phosphatase was subject to Tris-Tricine poly acrylamide gel (12.5%) electrophoresis as described above, and analyzed by immunoblotting with anti-human Aβ amino-terminal antibody 82E1 (1:5,000 dilution Cat 10,323, IBL, Fujioka, Japan). Protein size markers (WIDE-VIEW Prestained Protein Size Marker III, Cat 230–02,461, Fujifilm Wako, Tokyo, Japan) were used.

Detection and measurement of amyloid plaques in mouse brain

Indicated ages of APP-KI, APP-KI/Alcα-KO, and APP-KI/Alcβ-KO mice brains were fixed, sliced to prepare 315-µm thick coronal sections (− 2.8 to + 0.7 mm to bregma) and posted onto a slide glass. The 10 slices per brain with a 315-µm interval were further processed. The slices were incubated in methanol containing 0.3% (v/v) hydrogen peroxide, washed in PBS three times, and incubated in PBS containing 70% (w/v) formic acid for 1 min. The slices were subject to blocking in PBS containing 5% (v/v) heat-inactivated horse serum (5% HIHS/PBS) for 1 h and further incubated in 5% HIGS/PBS including 10 µg/ml of AffiniPure Fab Fragment Donkey Anti-Mouse IgG (H + L) (Cat 715–007-003, Jackson ImmunoResearch Laboratories, West Grove, PA, USA) for 2 h at room temperature. After washing with PBS, the slices were stained with mouse monoclonal anti-human Aβ 82E1 antibody (0.2 µg/ml in 5% HIcHS/PBS; Cat 10,323, IBL, Fujioka, Japan) to detect amyloid plaques and VECTASTAIN Elite ABC Standard Kit (Cat PK-6100, Vector Laboratories, Newark, CA, USA) as described previously[48]. The images were turned to black-to-white images with NIH ImageJ software by thresholding non-plaque signals after manually removing artifacts derived from edges or folds. The sum of the pixel numbers of still positively stained in each image was counted with ImageJ, and the resulting number was divided by the pixel number of the area occupied by the slices[48].

Primary cultured neurons and immunostaining of neuronal proteins

Mixed mouse cortical and hippocampal neurons were cultured for the indicated day (days in vitro in culture/div) using a modification of a previous method[63]. Briefly, the cortex and hippocampus of mice at embryonic day 15.5 were removed and neurons dissociated in a buffer containing papain (Cat LS003119 Worthington, Lakewood, NJ, USA). The cells were seeded at $1–3 \times 10^5$ cells on 12 mm glass coverslips (No. 1S thickness, Matsunami glass, Osaka, Japan) coated with poly-L-lysine hydrobromide (Cat P2636, Sigma-Aldrich) and cultured in Neurobasal Medium (Cat 21,103,049, Gibco/Thermo Fisher Scientific, Waltham, MA) containing 2% (v/v) B-27 Supplement (Cat 17,504,044 Invitrogen, South San Francisco, CA, USA), Glutamax I (4 mM, Cat 35,050,061, Gibco/Thermo Fisher Scientific), heat-inactivated horse serum (5% v/v, Cat 26,050,088, Gibco/Thermo Fisher Scientific), and penicillin plus streptomycin (Cat 35,050,061, Invitrogen/Thermo Fisher Scientific). A half volume of the culture medium was removed and replaced with fresh medium twice a week. To prevent the growth of glial cells, 5-Fluoro-2'-deoxyuridine (Cat F0503, Sigma-Aldrich, St. Louis, MO, USA) was added to the cultured medium for the first 3–4 days in vitro[71].

The neurons were then fixed with 4% paraformaldehyde in PBS, treated with 0.1% Triton X-100 in PBS, blocked with 4% bovine serum albumin/BSA in PBS, and incubated in primary antibodies for 12 h. Subsequently, neurons were incubated with Alexa Fluor 488-conjugated anti-rabbit and Alexa Fluor 568-conjugated anti-mouse IgG antibody. Fluorescent images were obtained using Nikon A1 confocal fluorescence microscope (Nikon, Tokyo, Japan). Protein colocalization rates of each protein and APP were calculated using the Coloc2 plugin in Fiji (ImageJ) software. This plugin calculates the pixel intensity correlation between the immunostained images of each protein and APP, expressed as Pearson's R value. Cells were prepared independently in two separate experiments, and for each preparation, six to seven images were obtained. All values were pooled and subjected to statistical analysis, with the number of independent biological replicates specified.

The following antibodies were used for immunostaining of proteins; rabbit polyclonal anti-APP cytoplasmic antibody G369 (affinity-purified IgG with APP cytoplasmic domain peptide)[52], mouse monoclonal anti-BACE1 3D5[72], anti-LAMP1 H4A3 (Santa Cruz sc-20011), anti-Rab7 (Abcam, ab50533), and anti-EEA1 (BD Bioscience, 610,457) antibodies.

Statistical analysis

Statistical differences were assessed using Student's *t*-test or one-way ANOVAs combined with the Tukey–Kramer post-hoc test for multiple comparisons (GraphPad Prism software, version 9.4.0). *P*-values < 0.05 were considered significant.

Data availability

All data generated or analysed during this study are included in this published article and its supplementary information files.

Received: 10 March 2024; Accepted: 5 August 2024
Published online: 09 August 2024

References

1. Masters, C. L. & Selkoe, D. J. Biochemistry of amyloid β-protein and amyloid deposits in Alzheimer disease. *Cold Spring Harb Perspect. Med.* **2**, a006262 (2012).
2. Mandelkow, E.-M. & Mandelkow, E. Biochemistry and cell biology of Tau protein in neurofibrillary degeneration. *Cold Spring Harb Perspect. Med.* **2**, a006247 (2012).
3. Haure-Mirande, J.-V., Audrain, M., Ehrich, M. E. & Gandy, S. Microglial TYROBP/CAP12 in Alzheimer's disease: Transduction of physiological and pathological signals across TREM2. *Mol. Neurodegener.* **17**, 55 (2022).
4. Selkoe, D. J. Alzheimer's disease. *Cold Spring Harb Perspect. Biol.* **3**, a004457 (2011).
5. Zhao, N. *et al.* Alzheimer's risk factors age, apoE genotype and sex drive distinct molecular pathways. *Neuron* **106**, 727–742 (2020).
6. Thinakaran, G. & Koo, E. H. Amyloid precursor protein trafficking, processing, and function. *J. Biol. Chem.* **283**, 29615–29619 (2008).
7. Sreiner, J. H., Fluher, R. & Haass, C. Intramembrane proteolysis by γ-secretase. *J Biol Chem* **283**, 29627–29631 (2008).
8. Mullan, M. *et al.* A pathogenic mutation for probable Alzheimer's disease in the APP gene at N-terminus of β-amyloid. *Nat Genet* **1**, 345–347 (1992).
9. Di Fede, G. *et al.* A recessive mutation in the APP gene with dominant-negative effect on amyloidogenesis. *Science* **323**, 1473–1477 (2009).
10. Zhou, L. *et al.* Amyloid precursor protein mutation E682K at the alternative β-secretase cleavage β'-site increase Aβ generation. *EMBO Mol. Med.* **3**, 291–302 (2011).
11. St George-Hyslop, P. H. Molecular genetics of Alzheimer's disease. *Biol. Psychiatry* **47**, 183–199 (2000).
12. Jonsson, T. *et al.* A mutation in APP protects against Alzheimer's disease and age-related cognitive decline. *Nature* **488**, 96–99 (2012).
13. Kimura, A., Hata, S. & Suzuki, T. Alternative selection of β-site APP-cleaving enzyme 1 (BACE1) cleavage sites in amyloid β-protein precursor (APP) harboring protective and pathogenic mutations within the Aβ sequence. *J. Biol. Chem.* **291**, 24041–24053 (2016).
14. Cole, S. L. & Vassar, R. The role of amyloid precursor protein processing by BACE1, the β-secretase Alzheimer's disease pathophysiology. *J. Biol. Chem.* **283**, 29621–29625 (2008).
15. Benilova, I., Karran, E. & De Strooper, B. The toxic Aβ oligomer and Alzheimer's disease: an emperor in need of clothes. *Nat. Neurosci.* **15**, 349–357 (2012).
16. Araki, Y. *et al.* The novel cargo Alcadein induces vesicle association of kinesin -1 motor components and activates axonal transport. *EMBO J.* **26**, 1475–1486 (2007).
17. Dumanis, S. *et al.* FE65 as a link between VLDLR and APP to regulate their trafficking and processing. *Mol. Neurodegener.* **7**, 9 (2012).
18. Small, S. A. & Gandy, S. Sorting through the cell biology of Alzheimer's disease: Intracellular pathways to pathogenesis. *Neuron* **52**, 15–31 (2006).
19. Suzuki, T. & Nakaya, T. Regulation of APP by phosphorylation and protein interactions. *J. Biol. Chem.* **283**, 29633–29637 (2008).
20. Tomita, S. *et al.* Interaction of a neuron-specific protein containing PDZ domains with Alzheimer's amyloid precursor protein. *J. Biol. Chem.* **274**, 2243–2254 (1999).
21. Sano, Y. *et al.* Enhanced amyloidogenic metabolism of the amyloid β-protein precursor in the X11L-deficint mouse brain. *J. Biol. Chem.* **281**, 37853–37860 (2006).
22. Saito, Y. *et al.* X11 proteins regulate the translocation of APP into detergent resistant membrane and suppress the amyloidogenic cleavage of APP by BACE in brain. *J. Biol. Chem.* **283**, 35763–35771 (2008).
23. Kondo, M. *et al.* Increased amyloidogenic processing of transgenic human APP in X11-like deficient mouse brain. *Mol. Neurodegener.* **5**, 35 (2010).
24. Motodate, R. *et al.* X11 and X11L proteins regulate the level of extrasynaptic glutamate receptors. *J. Neurochem.* **148**, 480–498 (2019).
25. Minami, S. S. *et al.* The cytoplasmic adaptor protein X11α and extracellular matrix protein Reelin regulate ApoE receptor 2 trafficking and cell movement. *FASEB J.* **24**, 58–69 (2010).
26. Stricker, N. L. & Huganir, R. L. The PDZ domains of mLin-10 regulate its trans-Golgi network targeting and the surface expression of AMPA receptors. *Neuropharmacol.* **45**, 837–848 (2003).

27. Glodowski, D. R. *et al.* Distinct LIN-10 domains are required for its neuronal function, its epithelial function, and its synaptic localization. *Mol. Biol. Cell* **16**, 1417–1425 (2005).
28. Motodate, R., Saito, Y., Hata, S. & Suzuki, T. Expression and localization of X11 family proteins in neurons. *Brain Res.* **1646**, 227–234 (2016).
29. Araki, Y. *et al.* Novel cadherin-related membrane proteins, Alcadeins, enhance the X11-like protein mediated stabilization of amyloid β-protein precursor metabolism. *J. Biol. Chem.* **278**, 49448–49458 (2003).
30. Araki, Y. *et al.* Coordinated metabolism of Alcadein and amyloid β-protein precursor regulates FE65-dependent gene transactivation. *J. Biol. Chem.* **279**, 24343–24354 (2004).
31. Hintsch, G. *et al.* The calsyntenins–a family of postsynaptic membrane proteins with distinct neuronal expression patterns. *Mol. Cell Neurosci.* **21**, 393–409 (2002).
32. Konecna, A. *et al.* Calsyntenin-1 docks vesicular cargo to kinesin-1. *Mol. Biol. Cell* **17**, 3651–3663 (2006).
33. Ludwig, A. *et al.* Calsyntenins mediate TGN exit of APP in a kinesin-1-dependent manner. *Traffic* **10**, 572–589 (2009).
34. Kawano, T. *et al.* A small peptide sequence is sufficient for initiating kinesin-1 activation through part of TPR region of KLC1. *Traffic* **13**, 834–848 (2012).
35. Takei, N. *et al.* Cytoplasmic fragment of Alcadein α generated by regulated intramembrane proteolysis enhances amyloid β-protein precursor (APP) transport into the late secretory pathway and facilitates APP cleavage. *J. Biol. Chem.* **290**, 987–995 (2015).
36. Vagnoni, A. *et al.* Calsyntenin-1 mediates axonal transport of the amyloid precursor protein and regulates Aβ production. *Hum. Mol. Genet.* **21**, 2845–2854 (2012).
37. Sobu, Y. *et al.* Phosphorylation of multiple sites within an acidic region of Alcadein α is required for kinesin-1 association and Golgi exit of Alcadein α cargo. *Mol. Biol. Cell* **28**, 3844–3856 (2017).
38. Nakano, Y. *et al.* Retinal ganglion cell loss in kinesin-1 cargo Alcadein α deficient mice. *Cell Dearth Dis.* **11**, 166 (2020).
39. Shiraki, Y. *et al.* Axonal transport of Frizzled5 by Alcadein α-containing vesicles is associated with kinesin-1. *Mol. Biol. Cell* **34**(ar110), 1–14 (2023).
40. Pettem, K. L. *et al.* The specific α-neurexin interactor calsyntenin-3 promote excitatory and inhibitory synapse development. *Neuron* **80**, 113–128 (2013).
41. Um, J. W. *et al.* Calsyntenins function as synaptogenic adhesion molecules in concert with neurexins. *Cell Rep.* **27**, 1096–1109 (2014).
42. Lu, Z. *et al.* Calsyntenin-3 molecular architecture and interaction with neurexin 1α. *J. Biol. Chem.* **289**, 34530–34542 (2014).
43. Hata, S. *et al.* Alcadein cleavages by amtloid β-precursor protein (APP) α- and γ-secretases generate small peptides p3-Alcs indicating Alzheimer disease-related γ-secretase dysfunction. *J. Biol. Chem.* **284**, 36024–36033 (2009).
44. Hata, S. *et al.* Brain p3-Alcβ peptide restores neuronal viability impaired by Alzheimer's amyloid β-peptide. *EMBO Mol. Med.* **15**, e17052 (2023).
45. Boraxbekk, C. J. *et al.* Investigating the influence of KIBRA and CLSTN2 genetic polymorphisms on cross-sectional and longitudinal measures of memory performance and hippocampal volume in order individuals. *Neuropsychologia* **78**, 10–17 (2015).
46. Lipina, T. V. *et al.* Cognitive deficits in calsyntenin-2-deficient mice associated with reduced GABAergic transmission. *Neuropsychopharmacol* **41**, 802–810 (2016).
47. Hata, S. *et al.* Alternative γ-secretase processing of γ-secretase substrates in common forms of mild cognitive impairment and Alzheimer disease: Evidence for γ-secretase dysfunction. *Ann. Neurol.* **69**, 1026–1031 (2011).
48. Gotoh, N. *et al.* Amyloidogenic processing of amyloid β protein precursor (APP) is enhanced in the brains of alcadein α-deficient mice. *J. Biol. Chem.* **295**, 9650–9662 (2020).
49. Saito, T. *et al.* Single *App* knock-in mouse models of Alzheimer's disease. *Nat. Neurosci.* **17**, 661–663 (2014).
50. Gandy, S. Systemically administrated alcadein peptide p3-Alcβ neutralizes brain Alzheimer's Aβ oligomers. *Trends Mol. Med.* **29**, 487–488 (2023).
51. Lichtenthaler, S. F. *et al.* Mechanism of the cleavage specificity of Alzheimer's disease γ-secretase identified by phenylalanine-scanning mutagenesis of the transmembrane domain of the amyloid precursor protein. *Proc. Natl. Acad. Sci. U S A* **96**, 3053–3058 (1999).
52. Oishi, M. *et al.* The cytoplasmic domain of the Alzheimer's amyloid precursor protein is phosphorylated at Thr654, Ser655 and Thr668 in adult rat brain and cultured cells. *Mol. Med.* **3**, 111–123 (1997).
53. Iijima, K. *et al.* Neuron-specific phosphorylation of Alzheimer's β-amyloid precursor protein by cyclin-dependent kinase 5. *J. Neurochem.* **75**, 1085–1091 (2000).
54. Hata, S. *et al.* Enhanced amyloid-β generation by γ-secretase complex in detergent-resistant membrane microdomain accompanied by the reduced cholesterol level. *Human Mol. Gene.* **29**, 382–393 (2020).
55. Kakuda, N. *et al.* Altered γ-secretase activity in mild cognitive impairment and Alzheimer's disease. *EMBO Mol. Med.* **4**, 344–352 (2012).
56. Kakuda, N. *et al.* γ-Secretase activity is associated with Braak senile plaque stages. *Am. J. Pathol.* **190**, 1323–1331 (2020).
57. Lee, J. H. *et al.* The neuronal adaptor protein X11α reduces Aβ levels in the brains of Alzheimer's APPswe Tg2576 transgenic mice. *J. Biol. Chem.* **278**, 47025–47029 (2003).
58. Lee, J. H. *et al.* The neuronal adaptor protein X11β reduces amyloid β-protein levels and amyloid plaque formation in the brains of transgenic mice. *J. Biol. Chem.* **279**, 49099–49104 (2004).
59. Michell, J. C. *et al.* X11β rescues memory and long-term protention deficitis in Alzheimer's disease APPswe Tg2576 mice. *Human Mol. Gennet.* **18**, 4492–4500 (2009).
60. Hata, S. *et al.* Multiple γ-secretase product peptides are coordinately increased in concentration in the CSF of a subpopulation of sporadic Alzheimer's disease subjects. *Mol. Neurodegener.* **7**, 16 (2012).
61. Konno, T. *et al.* Coordinate increase of γ-secretase reaction products in the plasma of some female Japanese sporadic Alzheimer's disease patients: Quantitative analysis with a new ELISA system. *Mol. Neurodegener.* **6**, 76 (2011).
62. Omori, C. *et al.* Increased levels of plasma p3-Alcα35, a major fragment of Alcadein α by γ-secretase cleavage Alzheimer's disease. *J. Alzheimers Dis.* **39**, 861–870 (2014).
63. Chiba, K. *et al.* Quantitative analysis of APP axonal transport in neurons: role of JIP1 in enhanced APP anterograde transport. *Mol. Biol. Cell* **25**, 3569–3580 (2014).
64. Stokin, G. B. *et al.* Axonopathy and transport deficits early in the pathogenesis of Alzheimer's disease. *Science* **307**, 1282–1288 (2005).
65. Gowrishankar, S., Yuan, P., Wu, Y. & Ferguson, S. M. Massive accumulation of luminal protease-deficient axonal lysosomes at Alzheimer's disease amyloid plaques. *Proc. Natl. Acad. Sci. U S A* **112**, E3699–E3708 (2015).
66. Hwang, J. *et al.* The role of lysosomes in a broad disease-modifying approach evaluated across transgenic mouse models of Alzheimer's disease and Parkinson's disease and models of mild cognitive impairment. *Int. J. Mol. Sci.* **20**, 4432 (2019).
67. Hata, S. *et al.* Decrease in p3-Alcβ37 and p3-Alcβ40, products of Alcadein β generated by γ-secretase cleavages, in aged monkeys and patients with Alzheimer's disease. *Alzheimers Dement (N Y)* **5**, 740–750 (2019).
68. Honda, K. *et al.* Accumulation of amyloid-β in the brain of mouse models of Alzheimer's disease is modified by their altered gene expression in the presence of human apoE isoforms during aging. *Neurobiol. Aging* **123**, 63–74 (2023).

69. Tomita, S., Kirino, Y. & Suzuki, T. Cleavage of Alzheimer's amyloid precursor protein (APP) by secretases occurs after O-glycosylation of APP in the protein secretory pathway. Identification of intracellular compartments in which APP cleavage occurs without using toxic agents that interfere with protein metabolism. *J. Biol. Chem.* **273**, 6277–6284 (1998).
70. Mizumaru, C. *et al.* Suppression of APP-containing vesicle trafficking and production of β-amyloid by AID/DHHC-12 protein. *J. Neurochem.* **111**, 1213–1224 (2009).
71. Hui, C. W., Zhang, Y. & Herrup, K. Non-neuronal cells are required to mediate the effects of neuroinflammation: Results from a neuron-enriched culture system. *PloS One* **11**, e0147134 (2016).
72. O'Connor, T. *et al.* Phaosphorylation of the translation initiation factor elF2a increase BACE1 levels and promotes amyloidogenesis. *Neuron* **60**, 988–1009 (2008).

Acknowledgements

This work was supported in part by JSPS KAKENHI Grant Number JP23K06840 (SH) and JP22K15270 (YS), and JP22K06597 (TY), the Naito Foundation (SH), the Japan Agency for Medical Research and Development JP23dk0207059 (TS). Advanced Prevention and Research Laboratory for Dementia, Graduate School of Pharmaceutical Sciences, Hokkaido University is supported by Japan Medical Leaf Co., Ltd. We thank Dr. Vassar for supplying the BACE1 antibody.

Author contributions

K.H., R.A. conducted studies of Figs. 2, 4 and 6, H.Ta., R.A., and T.Y. performed studies of Fig. 3, and S.H. conducted studies of Fig. 6. T.Sa. and T.C.S. provided $App^{NL\text{-}F/NL\text{-}F}$ mouse, T.Y. generated and provided Alcα-KO and Alcβ-KO mice, and Y.S. and T.Su. generated $App^{NL\text{-}F/NL\text{-}F}$/Alcα-KO and $App^{NL\text{-}F/NL\text{-}F}$/Alcα-KO mice**.** S.H., T.Y. and T.Su. designed the study, S.H., H.T., and Y.S. conducted statistical analyses, K.H., S.H. T.Y. and T.Su. prepared the figures and wrote the paper. K.A. supported the studies in the revised manuscript. All authors discussed the data obtained and conducted the preparation of the manuscript.

Competing interests

The authors declare no competing interests.

Additional information

Supplementary Information The online version contains supplementary material available at https://doi.org/10.1038/s41598-024-69400-9.

Correspondence and requests for materials should be addressed to T.Y. or T.S.